PNAS
www.pnas.org

Supplementary Information for

Mechanistic Approaches for Chemically Modifying the Coordination Sphere of Copper–Amyloid-β Complexes

Jiyeon Han, Hyuck Jin Lee, Kyu Yeon Kim, Geewoo Nam, Junghyun Chae, and Mi Hee Lim*

Email: miheelim@kaist.ac.kr

This PDF file includes:

www.pnas.org/cgi/doi/10.1073/pnas.1916944117

Supplementary Materials and Methods

Preparation of L1. 2-Thiophenecarboxaldehyde (0.098 mL, 1 mmol) was added into a solution of *N*,*N*-dimethyl-*p*-phenylenediamine (140 mg, 1 mmol) in EtOH (5 mL). After refluxing the solution for 1 h, the reaction mixture was cooled to room temperature. The solvent was removed under vacuum yielding an imine product (brown solid). Sodium borohydride ($NaBH_4$; 230 mg, 6 mmol) was added into a solution of the imine product (230 mg, 1 mmol) in CH_3OH (10 mL) at 0 °C. After 10 min, the reaction mixture was stirred at room temperature for 30 min. The reaction was quenched with H_2O and extracted with CH_2Cl_2 (3x). The combined organic phase was washed with brine (1x) and dried over anhydrous magnesium sulfate ($MgSO_4$). The crude compound was purified by column chromatography (SiO_2; EtOAc:hexanes = 1:3) yielding the product (130 mg, 54%; yellow solid). ^{1}H NMR [400 MHz, DMSO-d_6, δ (ppm)]: 7.33 (1H, dd, J = 1.2 Hz, J = 5.0 Hz), 7.01 (1H, dq, J = 3.6 Hz), 6.95 (1H, dd, J = 3.6 Hz, J = 5.0 Hz), 6.62-6.59 (2H, m), 6.58-6.54 (2H, m), 5.60-5.57 (1H, m), 4.36 (2H, d, J = 5.6 Hz), 2.70 (6H, s). ^{13}C NMR [100 MHz, DMSO-d_6, δ (ppm)]: 145.1, 143.2, 140.5, 126.6, 124.4, 124.2, 115.1, 113.8, 43.0, 41.7. HRMS (*m/z*): $[M + H]^+$ Calcd. for $C_{13}H_{17}N_2S$: 233.1112, found: 233.1099.

Preparation of L2. 2-(Bromomethyl)thiophene (62 mg, 0.4 mmol) was added dropwise to a solution of potassium hydroxide (KOH; 33 mg, 0.6 mmol) and 4-(dimethylamino)benzenethiol (30 mg, 0.2 mmol) in DMF/H_2O (2 mL/0.2 mL). The reaction mixture was stirred at room temperature for 24 h and then cooled to 0 °C. The reaction was quenched with H_2O and extracted with EtOAc (4x). The combined organic layer was dried over anhydrous $MgSO_4$ and concentrated under vacuum. The crude compound was purified by column chromatography (SiO_2; EtOAc:hexanes = 1:6) yielding the product (36 mg, 73%; yellow liquid). ^{1}H NMR [400 MHz, DMSO-d_6, δ (ppm)]: 7.36 (1H, dd, J = 5.1 Hz, J = 1.3 Hz), 7.22-7.18 (2H, m), 6.88 (1H, dd, J = 5.1 Hz, J = 3.4 Hz), 6.82-6.81 (1H, m), 6.66-6.62 (2H, m), 4.21 (2H, d, J = 0.7 Hz), 2.80 (6H, s). ^{13}C NMR [100 MHz, CD_3OD, δ (ppm)]: 150.5, 141.8, 134.4, 126.0, 125.7, 124.1, 120.1, 112.3, 39.2, 35.5. HRMS (*m/z*): $[M + H]^+$ Calcd. for $C_{13}H_{16}NS_2$: 250.0724, found: 250.0713.

Preparation of L3. 2-(Bromomethyl)pyridine hydrobromide (100 mg, 0.4 mmol) was added dropwise to a mixture of KOH (57 mg, 1 mmol) and 4-(dimethylamino)benzenethiol (30 mg, 0.2 mmol) in DMF/H_2O (3 mL/0.3 mL). The reaction mixture was stirred for 4 h at room temperature and then cooled to 0 °C. The mixture was diluted with H_2O and extracted with EtOAc (4x). The combined organic layer was dried over anhydrous $MgSO_4$ and concentrated under vacuum. The crude compound was purified by column chromatography (SiO_2; EtOAc:hexanes = 1:4) yielding the product (33 mg, 65%; yellow liquid). ^{1}H NMR [400 MHz, CD_3OD, δ (ppm)]: 8.40 (1H, ddd, J = 0.8 Hz, J = 4.8 Hz), 7.67 (1H, td, J = 7.6 Hz, J = 1.6 Hz), 7.25 (1H, ddd, J = 1.2 Hz), 7.22-7.14 (3H, m), 6.64-6.60 (2H, m), 4.01 (2H, s), 2.90 (6H, s). ^{13}C NMR [100 MHz, CD_3OD, δ (ppm)]: 159.8, 152.0, 149.5, 138.4, 136.0, 125.2, 123.4, 120.6, 113.9, 43.6, 40.6. HRMS (*m/z*): $[M + H]^+$ Calcd. for $C_{14}H_{17}N_2S$: 245.1112, found: 245.1099.

Parallel Artificial Membrane Permeability Assay Adapted for the Blood-Brain Barrier (PAMPA–BBB). PAMPA–BBB experiments were conducted employing the PAMPA Explorer kit (*p*ION Inc., Billerica, MA, USA) following previously reported protocols (1–3). Compounds (25 μM, 200 μL) in Prisma HT buffer (pH 7.4, *p*ION) were added to the wells of a donor plate (number of replicates = 12). The polyvinylidene fluoride (PVDF, 0.45 μM) filter membrane on the acceptor plate was coated with BBB-1 lipid formulation (5 μL, *p*ION).

The acceptor plate was then placed on the top of the donor plate. Brain sink buffer (BSB, 200 μL, *p*ION) was added to each well of the acceptor plate and was incubated for 4 h at room temperature without agitation. UV–vis spectra of the solutions in the reference, acceptor, and donor plates were measured by a microplate reader. The PAMPA Explorer software v. 3.5 (*p*ION) was used to calculate the $-\log P_e$ values for compounds. CNS± designations were assigned by comparison with compounds that were identified in the previous reports (4, 5).

Aβ Aggregation Experiments. $A\beta_{40}$ or $A\beta_{42}$ was dissolved in ammonium hydroxide [NH_4OH (aq); 1% v/v]. The resulting solution was lyophilized and stored at –80 °C. A stock solution of Aβ was then prepared by dissolving the lyophilized peptide with NH_4OH (1% v/v, 10 μL) and diluting with ddH_2O. All Aβ samples were prepared following the previously reported procedures (1–3, 6). The concentration of the peptide solution was determined by measuring the absorbance of the solution at 280 nm (ε = 1,450 $M^{-1}cm^{-1}$ for $A\beta_{40}$; ε = 1,490 $M^{-1}cm^{-1}$ for $A\beta_{42}$). The peptide stock solution was diluted to a final concentration of 25 μM in the Chelex-treated buffer [20 μM HEPES, pH 6.6 [for Cu(II) samples] or pH 7.4 (for metal-free samples), 150 μM NaCl]. For the inhibition studies, compounds [final concentration, 50 μM; 1% v/v DMSO; the stock solutions of compounds were prepared using DMSO due to their limited solubility in H_2O (for **L1** and **L3**, soluble at 150 μM in H_2O; for **L2**, insoluble even at approximately 15 μM in H_2O)] were added to the samples of Aβ (25 μM) in the absence and presence of a copper chloride salt ($CuCl_2$; 25 μM) followed by incubation at 37 °C with constant agitation for 24 h. For the disaggregation studies, Aβ (25 μM) was incubated with and without $CuCl_2$ (25 μM) for 24 h at 37 °C with constant agitation to generate preformed Aβ aggregates. The resulting peptide aggregates were then treated with compounds (50 μM) and incubated with constant agitation for an additional 24 h. For the experiments under anaerobic conditions, all samples were prepared following the same procedure described above for the aerobic samples in a N_2-filled glove box.

Electrospray Ionization–Mass Spectrometry (ESI–MS) and Tandem MS (ESI–MS^2). The experiments were performed following the previously reported methods (7–9). $A\beta_{40}$, α-synuclein, human islet amyloid polypeptide (hIAPP), or ubiquitin (100 μM) was incubated with compounds (500 μM; 1% v/v DMSO) and/or metal ions (100 μM) in 20 mM ammonium acetate, pH 7.2 at 37 °C without agitation. $CuCl_2$, $[Cu(CH_3CN)_4]PF_6$ (0.1% v/v CH_3CN), $FeCl_2$, $FeCl_3$, $Co(NO_3)_2{\cdot}nH_2O$, and $ZnCl_2$ were used as metal salts. Incubated samples were diluted by 10 fold with ddH_2O and then injected into the mass spectrometer. The capillary voltage, sampling cone voltage, and source temperature were set to 2.8 kV, 70 V, and 40 °C, respectively. The backing pressure was adjusted to 2.7 mbar. The ESI parameters and experimental conditions of tandem MS (ESI–MS^2) were the same as above. The collision-induced dissociation (CID) was conducted by applying the collision energy in the trap and adjusting the low mass (LM) resolution to 15. More than 200 spectra were obtained for each sample and averaged for the analysis.

Inductively Coupled Plasma–Mass Spectrometry (ICP–MS). **L1** (final concentration, 50 μM; 1% v/v DMSO) was added to the samples containing $A\beta_{40}$ (25 μM) and $CuCl_2$ (25 μM) in ddH_2O followed by incubation at 37 °C with constant agitation. After 24 h, the samples were centrifuged at 12,000 rpm for 30 min at 4 °C to obtain the supernatants. The Cu concentration in the supernatants was analyzed by the ICP–MS in duplicate.

Circular Dichroism (CD) Spectroscopy. $A\beta_{40}$ (25 μM) and $Cu(NO_3)_2 \cdot nH_2O$ (25 μM) were incubated in ddH_2O for 24 h with or without **L1** (50 μM; 0.1% v/v DMSO). The CD spectra of Aβ samples were collected between 190 and 260 nm with a cell path length of 0.5 mm. The digital integration time, bandwidth, and scanning speed were 4 s, 2 nm, and 20 nm/min, respectively. Each spectrum was smoothed by a Fourier transform. Following the previously reported method (10), the change in the secondary structures of Cu(II)–$A\beta_{40}$ with treatment of **L1** was analyzed.

Cyclic Voltammetry. Cyclic voltammograms of **L1**–**L3** (dissolved in DMSO; final concentration, 1 mM) were recorded in 0.1 M *tetra-N*-butylammonium perchlorate (in DMSO) and 1 M NaCl (in ddH_2O; 1% v/v DMSO) at various scan rates (25, 50, 100, 150, 200, and 250 mV/s) at room temperature. A three-electrode setup is composed of an Ag/Ag(I) reference electrode [RE-1B reference electrode Ag/Ag(I); Qrins, Seoul, Republic of Korea], a Pt wire auxiliary electrode (SPTE platinum electrode; Qrins), and a glassy carbon working electrode (Qrins).

Gel Electrophoresis with Western Blotting (Gel/Western Blot). The resultant Aβ species from in vitro experiments were analyzed by the gel/Western blot using an anti-Aβ antibody (6E10) (1–3, 6). The samples (10 μL) were separated on a 10-20% Tris-tricine gel (Thermo Fisher Scientific, Waltham, MA, USA). Following the separation, the proteins were transferred onto nitrocellulose membranes and blocked with bovine serum albumin (BSA, 3% w/v, Sigma-Aldrich, St. Louis, MO, USA) in Tris-buffered saline (TBS) containing 0.1% Tween-20 (TBS-T) for 2 h (at room temperature) or overnight (at 4 °C). The membranes were incubated with 6E10 (1:2,000, Covance, Princeton, NJ, USA) in the solution of BSA (2% w/v in TBS-T) for 4 h (at room temperature) or overnight (at 4 °C). After washing with TBS-T (3x, 10 min), a horseradish peroxidase-conjugated goat anti-mouse secondary antibody (1:5,000 in 2% w/v BSA in TBS-T; Cayman Chemical Company, MI, USA) was added for 1.5 h at room temperature. A homemade ECL kit was used to visualize gel/Western blots on a ChemiDoc MP Imaging System (Bio-Rad, Hercules, CA, USA) (7, 8, 11).

Transmission Electron Microscopy (TEM). Samples for TEM were prepared following the previously reported methods (1–3, 6–8). Glow-discharged grids (Formvar/Carbon 300-mesh, Electron Microscopy Sciences, Hatfield, PA, USA) were treated with Aβ samples (25 μM, 5 μL) for 2 min at room temperature. Excess sample was removed using filter paper followed by washing twice with ddH_2O. Each grid incubated with uranyl acetate (1%, ddH_2O, 5 μL) for 1 min was blotted off and dried for 15 min at room temperature. Images for each sample were taken on a JEOL JEM-2100 transmission electron microscope (200 kV; 25,000x magnification).

Dot Blot Assay. To verify the effect of **L1** on oligomerization of Cu(II)–$A\beta_{40}$, the samples containing $A\beta_{40}$ (100 μM) and $CuCl_2$ (100 μM) with and without **L1** (200 μM), prepared and incubated for 24 h in 20 mM HEPES, pH 6.6, 150 mM NaCl, were analyzed by a dot blot assay. Moreover, to analyze the modified region of Aβ by hydrogen peroxide (H_2O_2), a dot blot assay was performed using the 1 and 24 incubated samples of $A\beta_{40}$ (100 μM) with or without $CuCl_2$ (100 μM) in the absence and presence of H_2O_2 (5 mM) in 20 mM ammonium acetate, pH 7.2. The resulting solution (5 μL) was spotted on a nitrocellulose membrane and blocked with a BSA solution (3% w/v) in 0.01% TBS-T at room temperature for 12 h. The membrane was incubated with a primary antibody [6E10 (1:2,000), A11 (1:1,000;

Invitrogen, Carlsbad, CA, USA), OC (1:2,000; Merch Millipore, Billerica, MA, USA), or anti-$A\beta_{40}$ (1:2,000; Abcam, Cambridge, UK)] in the solution of BSA (2% w/v in TBS-T) for 4 h at room temperature. After washing with 0.01% TBS-T (3x, 7 min), the horseradish peroxidase-conjugated goat anti-mouse (1:5,000; for 6E10 and anti-$A\beta_{40}$) or goat anti-rabbit (1:4,000; for A11 and OC) secondary antibody in the solution of BSA (2% w/v in TBS-T) was added to the membrane and incubated for 2 h at room temperature. A homemade ECL kit was used to visualize the results on a ChemiDoc MP Imaging System (7, 8, 11).

Cell Viability Studies. The human neuroblastoma SH-SY5Y cell line was purchased from the American Type Culture Collection (ATCC, VA, USA). The cell line was maintained in media containing 50% minimum essential medium (MEM) and 50% F12 (GIBCO, NY, USA), and supplemented with 10% fetal bovine serum (Sigma-Aldrich), 100 U/mL penicillin, and 100 mg/mL streptomycin (GIBCO). Cells were grown and maintained at 37 °C in a humidified atmosphere with 5% CO_2. The cells used for our studies did not indicate mycoplasma contamination. Cell viability upon treatment with compounds was determined by the MTT assay. $A\beta_{40}$ or $A\beta_{42}$ (50 μM) and $CuCl_2$ (50 μM) were pre-incubated with or without compounds (50 μM; 1% v/v DMSO) for 24 h at 37 °C with constant agitation. Cells were seeded in a 96 well plate (10,000 cells in 100 μL per well) and treated with the resultant samples (final concentration of 10 μM). After 24 h incubation, MTT [25 μL of 5 mg/mL in PBS (pH 7.4, GIBCO)] was added to each well, and the plate was incubated for 4 h at 37 °C. Formazan produced by cells was solubilized using an acidic solution of DMF (pH 4.5, 50% v/v, aq) and sodium dodecyl sulfate (SDS; 20% w/v) overnight at room temperature in the dark. The absorbance was measured at 600 nm by a microplate reader. Cell viability was calculated relative to that of the cells containing an equivalent amount of DMSO.

Trolox Equivalent Antioxidant Capacity (TEAC) Assay. The ability of compounds to scavenge free organic radicals in EtOH was determined by the assay according to a previously reported method with slight modifications (1, 7). To generate blue ABTS cation radicals [$ABTS^{+\bullet}$; ABTS = 2,2'-azino-bis(3-ethylbenzothiazoline-6-sulfonic acid) diammonium salt; Sigma-Aldrich], ABTS (7.0 mM, Sigma-Aldrich) with potassium persulfate [$K_2(SO_4)_2$; 2.5 mM] was dissolved in ddH_2O (5 mL) and incubated for 16 h in the dark at room temperature. The resulting solution of $ABTS^{+\bullet}$ was diluted with EtOH to absorbance of approximately 0.7 at 734 nm. The solution of $ABTS^{+\bullet}$ (200 μL) was added to the wells of a clear 96 well plate. Our compounds and Trolox (Trolox = 6-hydroxy-2,5,7,8-tetramethyl-chroman-2-carboxylic acid) were dissolved in EtOH and treated to the solution of $ABTS^{+\bullet}$. The final concentrations (2.1, 4.3, 6.4, 8.6, 11, and 16 μM) of compounds and Trolox were used. After 10 min incubation at room temperature, the absorbance at 750 nm was recorded. The percent inhibition was calculated according to the measured absorbance [% inhibition = $100 \times (A_0 - A)/A_0$, where A and A_0 are the absorbance of the samples with and without compound treatment, respectively] and was plotted as a function of compound concentration. The TEAC values of compounds for each time point were calculated as a ratio of their slope to that of Trolox.

H_2O_2/Peroxidase Assay. The ability of **L1** to quench H_2O_2 was evaluated using an Amplex Red H_2O_2/peroxidase assay kit (Thermo Fisher Scientific). Following the manufacturer's procedure with minor modifications, **L1** (final concentration, 5, 50, and 500 μM; 1% v/v DMSO) and an equivalent amount of DMSO (1% v/v) were treated to a solution of H_2O_2 (50 μM) in a 96 well plate. In addition, to evaluate the effect of **L1** on the Cu(I/II)–

Aβ-mediated production of reactive oxygen species, **L1** (final concentration, 50 μM; 1% v/v DMSO) was incubated with $A\beta_{40}$ (25 μM), $CuCl_2$ (25 μM), and *L*-ascorbate (1 mM; Sigma-Aldrich). Upon addition of the working solution containing Amplex Red (25 μM) and horseradish peroxidase (1 U/mL) in 50 mM sodium phosphate buffer, pH 7.4, the plate was incubated at room temperature for 30 min. The absorbance of resorufin, a red chromophore product from Amplex Red, was measured at 590 nm. The amount of resultant H_2O_2 was determined based on the standard curve that was obtained using various concentrations of H_2O_2 (0, 5, 10, 15, 20, 25, 30, 35, 40, 50, and 70 μM).

Scheme S1. Synthetic routes to **L1**–**L3**.

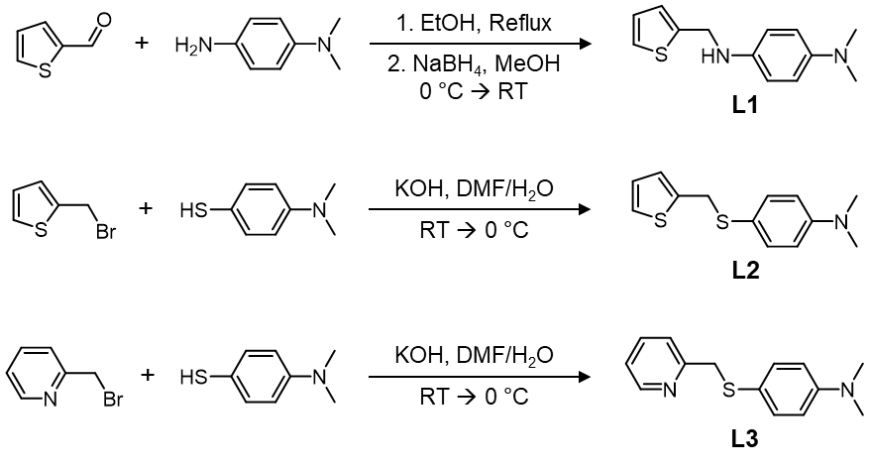

Table S1. Values (MW, clog*P*, HBA, HBD, PSA, logBB, and $-\log P_e$) of **L1**–**L3**.

	L1	**L2**	**L3**	Lipinski's Rules and Others
MW[a]	232	249	244	≤ 450
*c*log*P*[b]	15.3	4.08	2.94	≤ 5
HBA[c]	2	1	2	≤ 10
HBD[d]	1	0	0	≤ 5
PSA (Å^2)[e]	15.3	3.24	16.1	≤ 90
logBB[f]	0.345	0.702	0.338	< –1.0 (poorly)
$-\log P_e$[g]	4.31 ± 0.13 (CNS+)	4.61 ± 0.22 (CNS+)	4.35 ± 0.07 (CNS+)	$-\log P_e$ < 5.4 (CNS+) $-\log P_e$ > 5.7 (CNS–)

[a]MW, molecular weight; [b]clog*P*, calculated log of water-octanol partition coefficient; [c]HBA, hydrogen bond acceptor atom; [d]HBD, hydrogen bond donor atom; [e]PSA, polar surface area; [f]logBB, logarithm of the ratio of the concentration of the compound in the brain to concentration in the blood, $0.152 \times c\log P - 0.0148 \times \mathrm{PSA} + 0.139$; [g]$-\log P_e$, the value obtained using the PAMPA–BBB assay with the PAMPA Explorer software v. 3.5. Compounds assigned to be CNS+ are able to penetrate the BBB and thus be available in the central nervous system (CNS).

Table S2. Quantitative data of the cyclic voltammograms of compounds in DMSO.

Scan rate (mV/s)	L1		L2		L3	
	E_{pa} (V)	i_{pa} (μA)	E_{pa} (V)	i_{pa} (μA)	E_{pa} (V)	i_{pa} (μA)
25	0.21	7.2	0.72	19	0.73	23
50	0.23	14	0.73	26	0.75	32
100	0.24	19	0.75	39	0.76	45
150	0.25	20	0.76	48	0.77	49
200	0.26	26	0.76	49	0.78	57
250	0.27	42	0.77	53	0.79	61

Table S3. Quantitative data of the cyclic voltammograms of compounds in H_2O.[a]

Scan rate (mV/s)	L1			
	E_{pa} (V)	i_{pa} (μA)	E_{pc} (V)	i_{pc} (μA)
25	0.116	2.6	0.0793	0.11
50	0.117	4.0	0.0793	0.34
100	0.120	5.7	0.0778	0.37
150	0.124	9.3	0.0778	1.0
200	0.129	12	0.0780	1.6
250	0.129	15	0.0780	1.6
Scan rate (mV/s)	L3			
	E_{pa} (V)	i_{pa} (μA)	E_{pc} (V)	i_{pc} (μA)
25	0.534	4.9	0.484	2.7
50	0.538	7.0	0.483	4.2
100	0.539	11	0.483	6.3
150	0.540	13	0.483	7.8
200	0.540	16	0.483	9.5
250	0.543	21	0.480	11

[a]Note that the redox potential of **L2** could not be measured in H_2O due to its limited solubility.

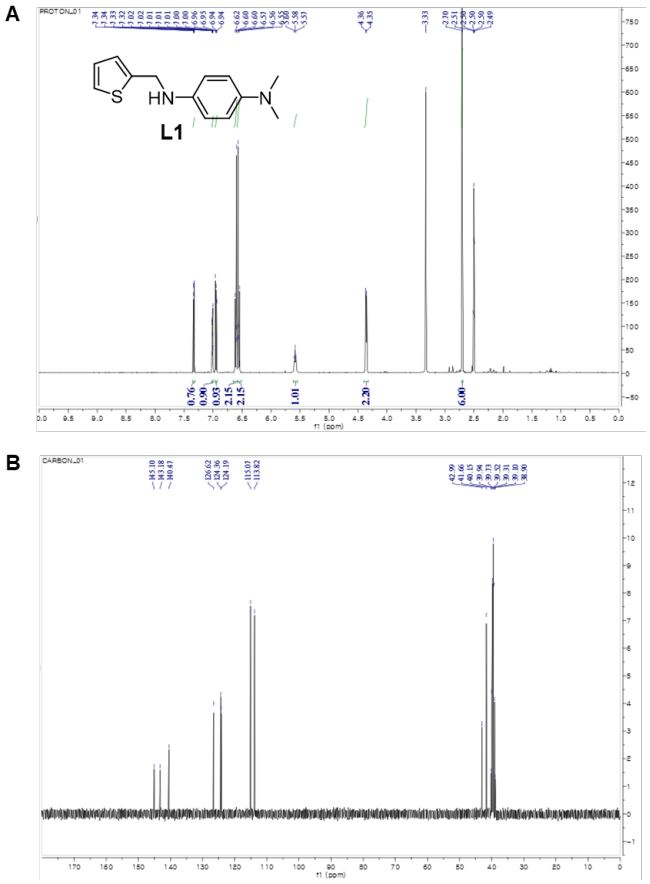

Fig. S1. ^{1}H (*A*, 400 MHz) and ^{13}C (*B*, 100 MHz) NMR spectra of **L1** in DMSO-d_6.

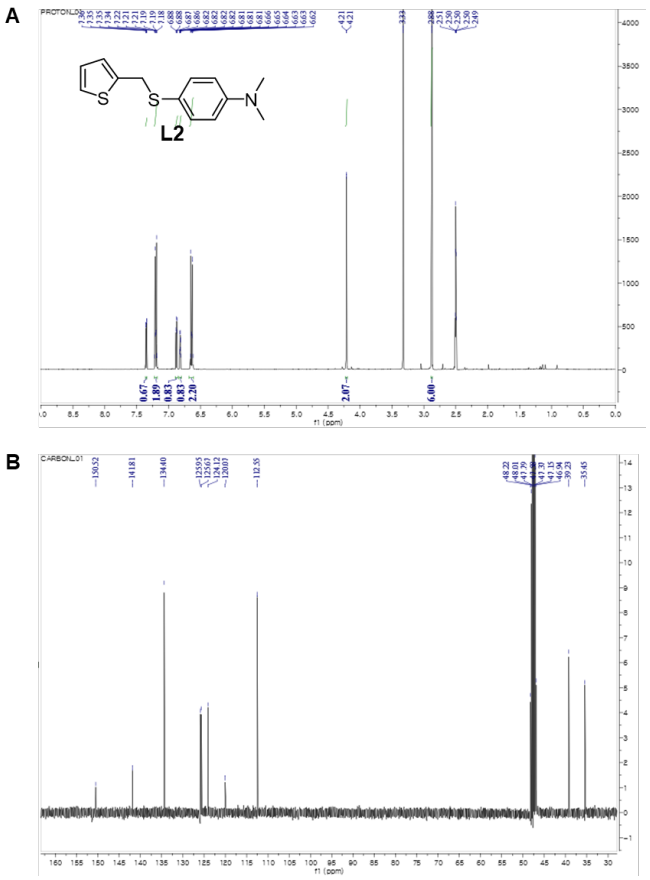

Fig. S2. ^{1}H (*A*, 400 MHz) and ^{13}C (*B*, 100 MHz) NMR spectra of **L2** in DMSO-d_6 and CD_3OD, respectively.

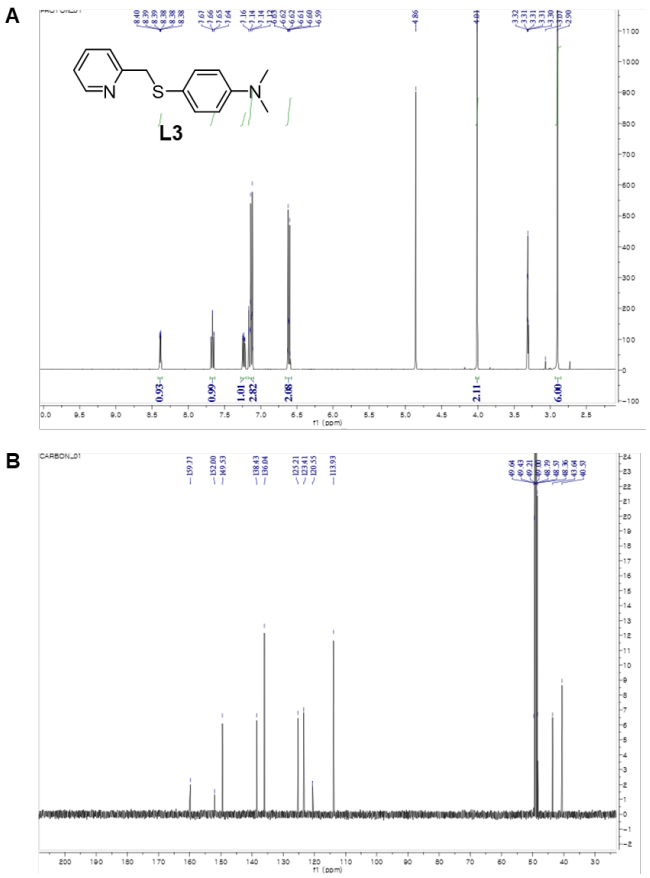

Fig. S3. ^{1}H (*A*, 400 MHz) and ^{13}C (*B*, 100 MHz) NMR spectra of **L3** in CD_3OD.

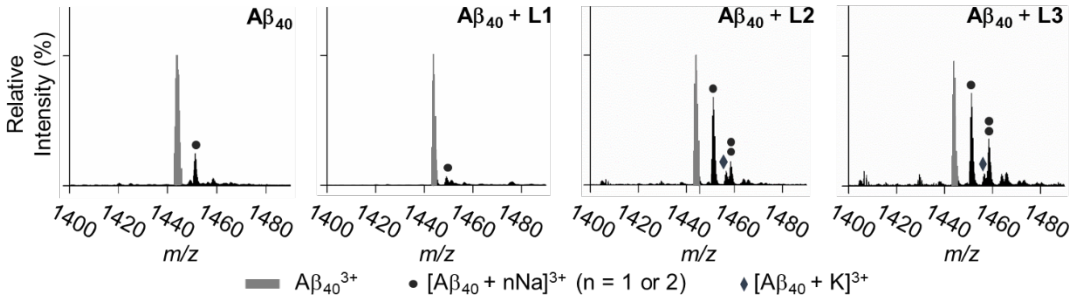

Fig. S4. Interaction of **L1**–**L3** with metal-free $A\beta_{40}$, analyzed by ESI–MS. Na^+ and K^+ adducts of $A\beta_{40}$ are marked with black dots and diamonds, respectively. Conditions were as follows: [$A\beta_{40}$] = 100 μM; [compound] = 500 μM; incubation for 3 h; 20 mM ammonium acetate, pH 7.2; 37 °C; no agitation. The samples were diluted with H_2O by 10 fold prior to injection to the mass spectrometer.

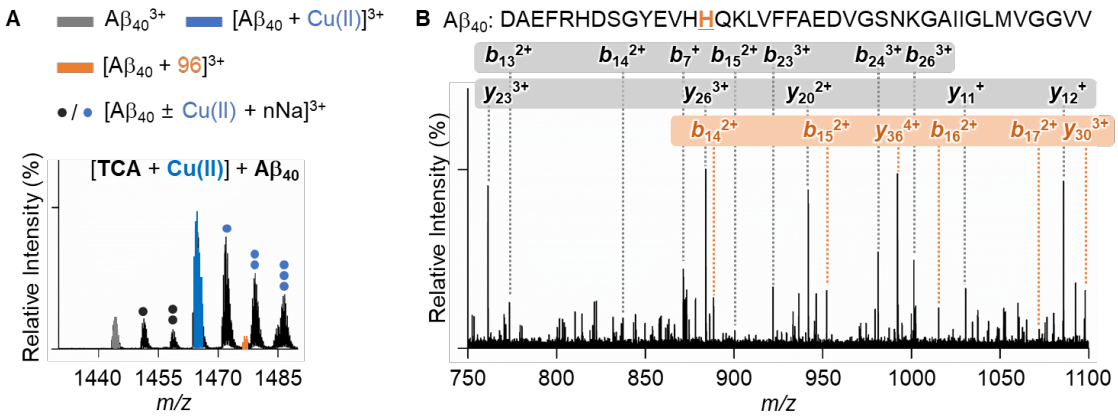

Fig. S5. Analysis of Cu(II)-added Aβ$_{40}$ upon treatment with **TCA** by ESI–MS. (*A*) ESI–MS spectrum of the +3-charged Cu(II)-added Aβ$_{40}$ monomer incubated with **TCA**. The peak of the covalent adduct between Aβ$_{40}$ and 2-methylthiophene (1,475 *m/z*) is indicated in orange. Na^+ adducts of Aβ$_{40}$ with or without Cu(II) are shown with blue and black dots. (*B*) ESI–MS^2 spectrum of the covalent adduct (1,475 *m/z*). The gray and orange boxes indicate b_x and y_x fragments corresponding to Aβ and Aβ bound to 2-methylthiophene, respectively. Conditions were as follows: [Aβ$_{40}$] = 100 μM; [$CuCl_2$] = 100 μM; [**TCA**] = 500 μM; incubation for 1 h; 20 mM ammonium acetate, pH 7.2; 37 °C; no agitation. The sample was diluted with H_2O by 10 fold prior to injection to the mass spectrometer.

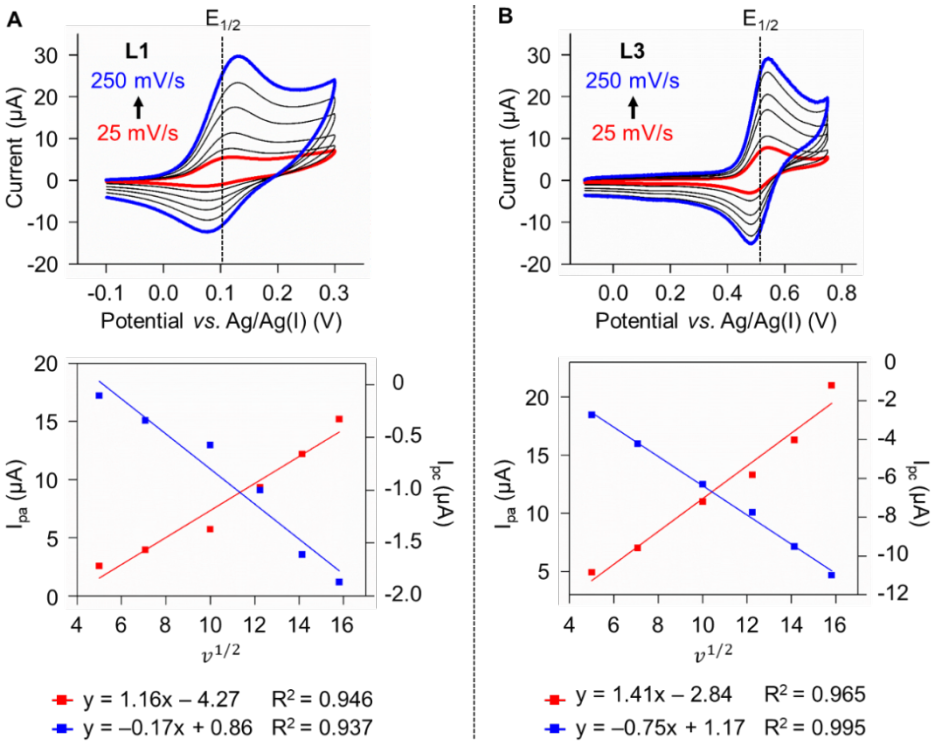

Fig. S6. Cyclic voltammograms of **L1** and **L3** in H_2O. The dashed black line indicates the $E_{1/2}$ value of compounds. (*A* and *B*) Plots of the current (i_{pa} and i_{pc}) as a function of scan rate ($\nu^{1/2}$) show the quasi-reversible and reversible couples of **L1** and **L3**, respectively. Note that the cyclic voltammogram of **L2** in H_2O could not be obtained due to its limited solubility. Conditions were as follows: [compound] = 1 mM; 1 M NaCl (aq); various scan rates [25 (red), 50, 100, 150, 200 and 250 (blue) mV/s]; room temperature; three electrodes composed of the glassy carbon working electrode, platinum counter electrode, and Ag/Ag(I) reference electrode.

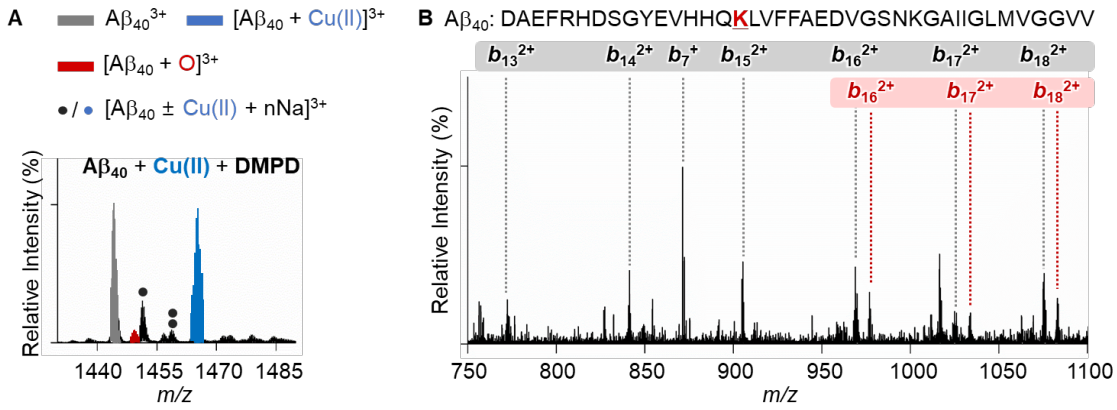

Fig. S7. Analysis of the oxidized $A\beta_{40}$ by treatment of **DMPD** through ESI–MS. (*A*) ESI–MS spectum of the +3-charged Cu(II)-added $A\beta_{40}$ monomer incubated with **DMPD**. (*B*) ESI–MS^2 spectrum of the singly oxidized $A\beta_{40}$ produced upon addition of **DMPD**. Chemical bonds of the selected ion at 1,449 *m/z* are cleaved by CID. The gray and red boxes indicate b_x fragments corresponding to Aβ and oxidized Aβ, respectively. Conditions were as follows: [$A\beta_{40}$] = 100 μM; [$CuCl_2$] = 100 μM; [**DMPD**] = 500 μM; incubation for 1 h; 20 mM ammonium acetate, pH 7.2; 37 °C; no agitation. The sample was diluted with H_2O by 10 fold prior to injection to the mass spectrometer.

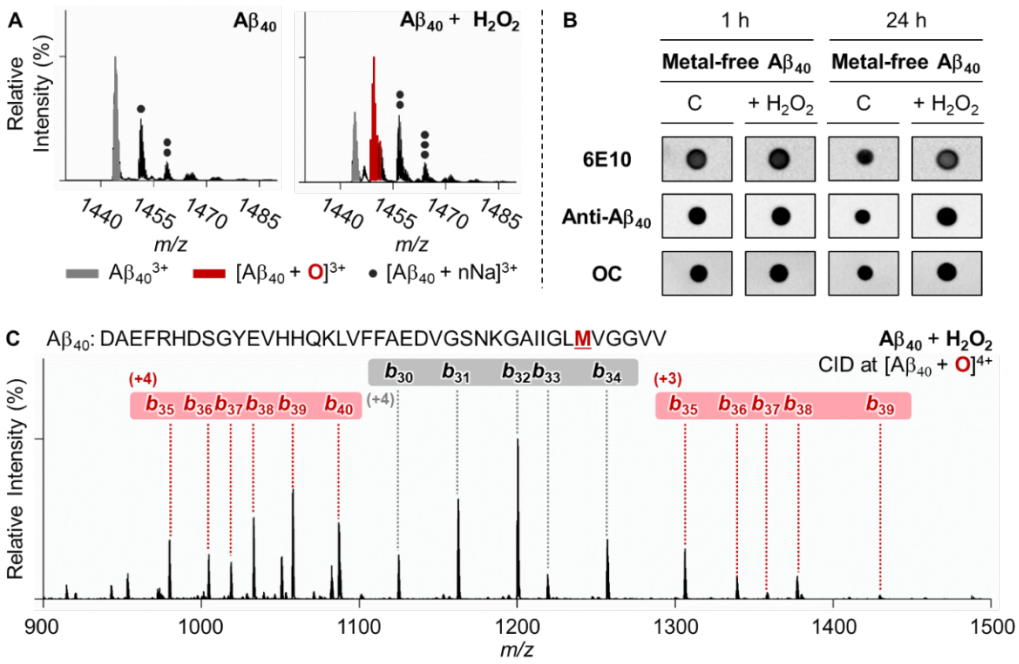

Fig. S8. Analysis of metal-free $A\beta_{40}$ by treatment of H_2O_2. (*A*) ESI–MS spectra of the +3-charged $A\beta_{40}$ monomer incubated with and without H_2O_2. (*B*) Dot blots of the metal-free $A\beta_{40}$ obtained upon incubation with H_2O_2. The epitopes of 6E10 and anti-$A\beta_{40}$ antibodies are the N- and C-termini of $A\beta_{40}$, respectively. The OC antibody was used to detect $A\beta_{40}$ fibrils. (*C*) ESI–MS^2 spectrum of the singly oxidized $A\beta_{40}$ generated by H_2O_2. Chemical bonds of the selected ion at 1,449 *m/z* were cleaved by CID. The gray and red boxes indicate b_x fragments corresponding to Aβ and oxidized Aβ, respectively. Conditions were as follows: [$A\beta_{40}$] = 100 μM; [H_2O_2] = 5 mM; incubation for 1 or 24 h; 20 mM ammonium acetate, pH 7.2; 37 °C; no agitation. The samples were diluted with H_2O by 10 fold prior to injection to the mass spectrometer.

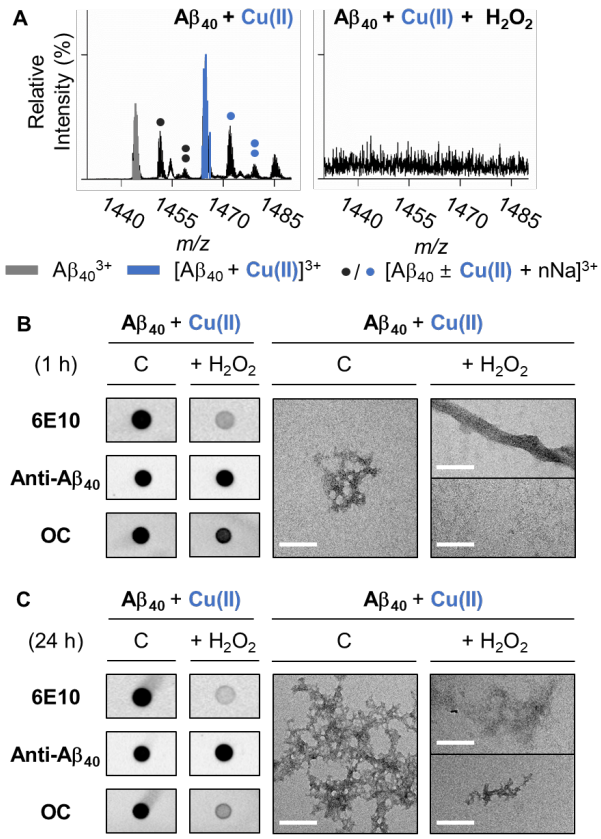

Fig. S9. Analysis of Cu(II)-treated Aβ$_{40}$ treated with H_2O_2. (*A*) ESI–MS spectra of the +3-charged Cu(II)–Aβ$_{40}$ monomer incubated with and without H_2O_2. (*B* and *C*) Dot blots and TEM images of Cu(II)-added Aβ$_{40}$ species produced by treatment of H_2O_2. The epitopes of 6E10 and anti-Aβ$_{40}$ antibodies are the N- and C-termini of Aβ$_{40}$, respectively. The OC antibody was used to detect Aβ$_{40}$ fibrils. Scale bars (for TEM), 200 nm. Conditions were as follows: [Aβ$_{40}$] = 100 μM; [$CuCl_2$] = 100 μM; [H_2O_2] = 5 mM; incubation for 1 or 24 h; 20 mM ammonium acetate, pH 7.2; 37 °C; no agitation. The samples were diluted with H_2O by 10 fold prior to injection to the mass spectrometer.

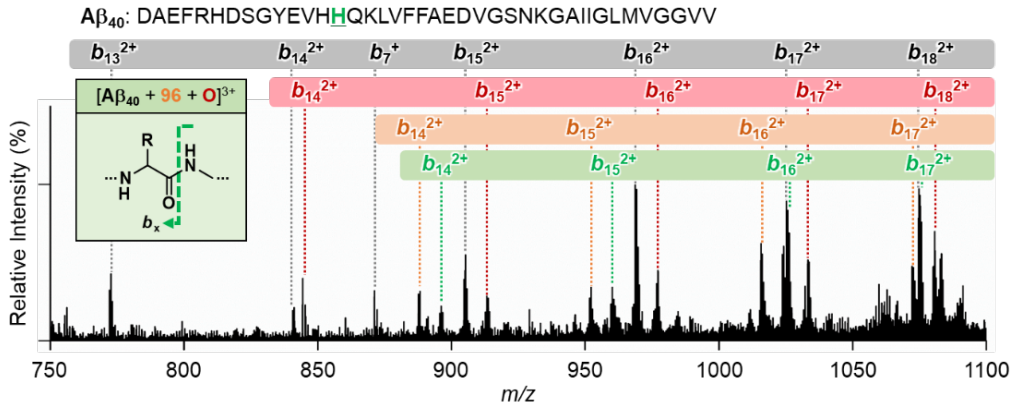

Fig. S10. ESI–MS^2 spectrum of the singly oxidized covalent $A\beta_{40}$ adduct, $[A\beta_{40} + 96 + O]^{3+}$, detected at 1,480 *m/z* in Fig. 2*A*. The gray, red, orange, and green boxes indicate b_x fragments corresponding to Aβ, oxidized Aβ, Aβ bound to 2-methylthiophene, and oxidized Aβ bound to 2-methylthiophene, respectively. Conditions were as follows: $[A\beta_{40}]$ = 100 μM; $[CuCl_2]$ = 100 μM; [**L1**] = 500 μM; incubation for 1 h; 20 mM ammonium acetate, pH 7.2; 37 °C; no agitation. The samples were diluted with H_2O by 10 fold prior to injection to the mass spectrometer.

A

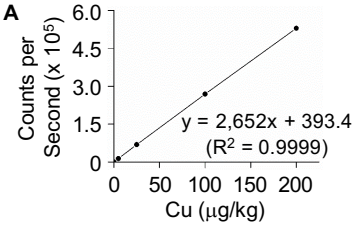

B

Samples	Cu (μg/kg)	Cu (μM)
Cu(II)	1570	24.7
$A\beta_{40}$ + Cu(II)	21.3	0.337
$A\beta_{40}$ + Cu(II) + **L1**	1190	18.7

Fig. S11. Concentration of copper in the supernatants of samples, measured by ICP–MS. (*A* and *B*) The amount of copper was determined by the standard curve that was obtained using its various concentrations (0, 5, 25, 100 and 200 μM). Conditions were as follows: [$A\beta_{40}$] = 25 μM; [$CuCl_2$] = 25 μM; [compound] = 50 μM; 24 h incubation; 37 °C; constant agitation; centrifugation at 12,000 rpm at 4 °C to obtain the supernatants of samples.

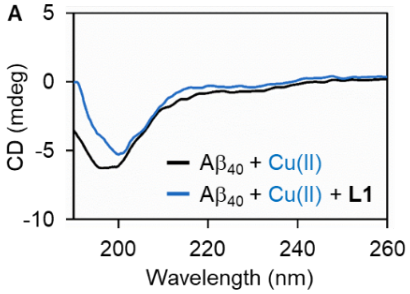

B

Secondary Structure (%)		
	$A\beta_{40}$ + Cu(II)	+ **L1**
α-Helix	6.1	0
β-Strand	26	34
Turn	18	17
Random Coils	50	49

Fig. S12. Change in the secondary structures of Cu(II)-treated $A\beta_{40}$ upon treatment of **L1**, monitored by CD spectroscopy. (*A*) CD spectra of the Cu(II)-added $A\beta_{40}$ samples incubated with or without **L1**, presented in the blue and black lines, respectively. (*B*) Analysis of the secondary structures of the samples from (*A*). Conditions were as follows: [$A\beta_{40}$] = 25 μM; [Cu(II)] = 25 μM; [**L1**] = 50 μM; incubation for 24 h; H_2O; 37 °C; constant agitation.

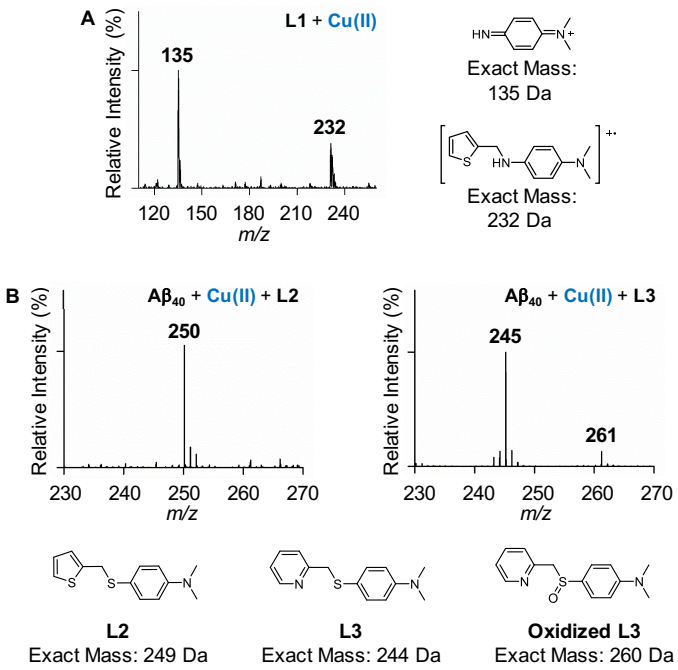

Fig. S13. Transformation of **L1**–**L3** in the presence of Cu(II) and/or Aβ_{40}, analyzed by ESI–MS. (*A*) Cu(II)-mediated transformation of **L1**, monitored by ESI–MS. The fragmentation and oxidation of **L1** were observed at 135 and 232 *m/z*, respectively. (*B*) ESI–MS spectra of **L2** and **L3** upon incubation with Aβ_{40} and Cu(II). The oxidation of **L3** was indicated at 261 *m/z*. Conditions were as follows: [Aβ_{40}] = 100 μM; [$CuCl_2$] = 100 μM; [compound] = 500 μM; incubation for 1 h; 20 mM ammonium acetate, pH 7.2; 37 °C; no agitation. The samples were diluted with H_2O by 10 fold prior to injection to the mass spectrometer.

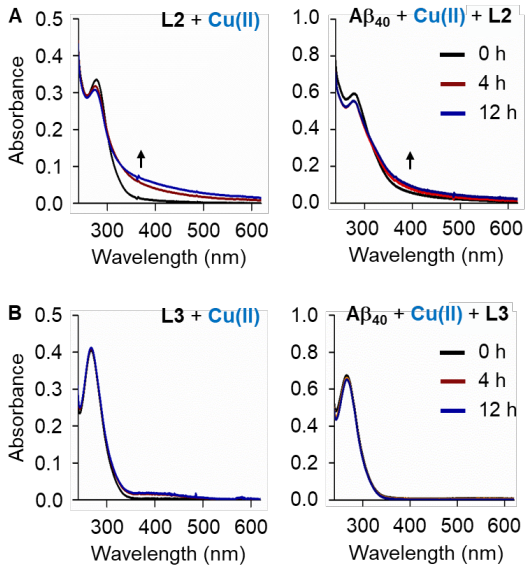

Fig. S14. Change of **L2** and **L3** in the presence of Cu(II) with or without $A\beta_{40}$, analyzed by UV–vis. (*A* and *B*) Optical spectra of **L2** and **L3** in the presence of Cu(II) upon incubation with or without $A\beta_{40}$ for 0, 4, and 12 h. Conditions were as follows: [$A\beta_{40}$] = 25 μM; [$CuCl_2$] = 25 μM; [**L2** or **L3**] = 50 μM; room temperature; incubation for 1 (black), 4 (orange), and 12 h (blue).

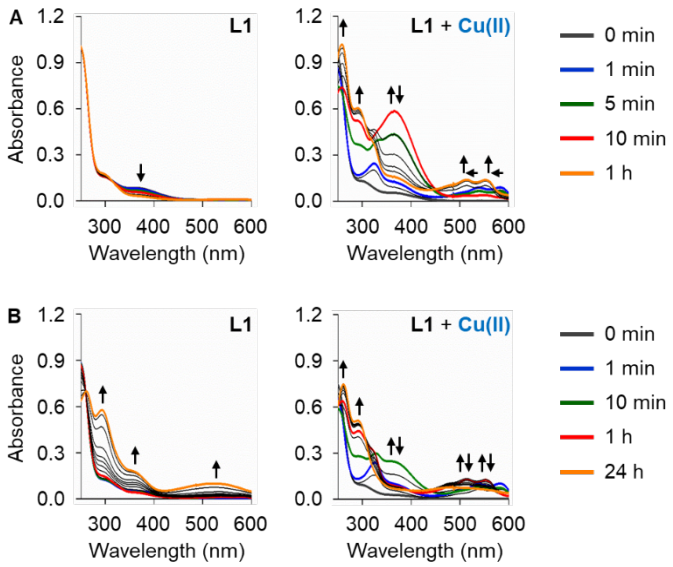

Fig. S15. Stability of **L1** under the experimental conditions presented in this study. Optical spectra of **L1** were recorded in the absence and presence of Cu(II). Conditions were as follows: (*A*) for ESI–MS: [**L1**] = 50 μM; [$CuCl_2$] = 10 μM; 20 mM ammonium acetate, pH 7.2; 37 °C; incubation for 1 h; (*B*) for gel/Western blot: [**L1**] = 50 μM; [$CuCl_2$] = 25 μM; 20 μM HEPES, 150 μM NaCl; 37 °C; incubation for 24 h.

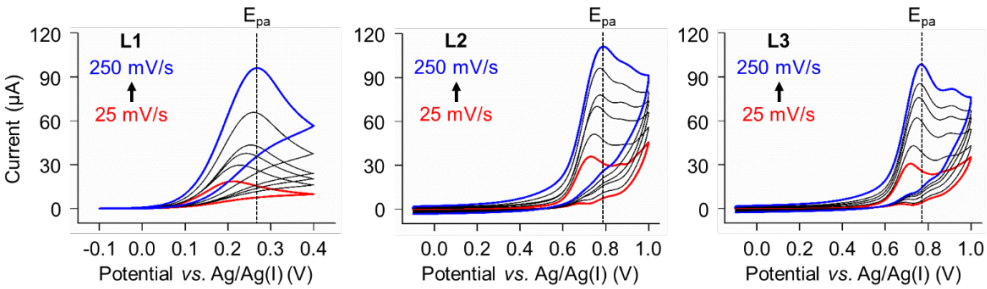

Fig. S16. Cyclic voltammograms of **L1**–**L3** at various scan rates in DMSO. The dashed black line indicates the anodic peak potential (E_{pa}) of compounds at 250 mV/s. Conditions were as follows: [compound] = 1 mM; 0.1 M *tetra-N*-butylammonium perchlorate; various scan rates [25 (red), 50, 100, 150, 200 and 250 (blue) mV/s]; room temperature; three electrodes composed of the glassy carbon working electrode, platinum counter electrode, and Ag/Ag(I) reference electrode.

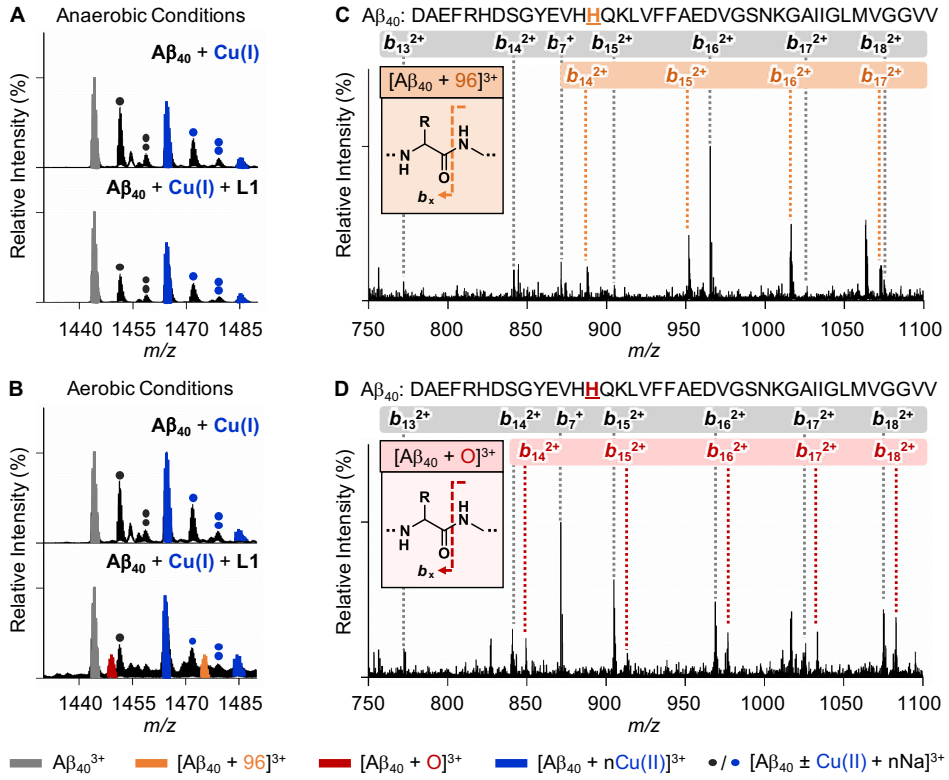

Fig. S17. Interaction of **L1** with Cu(I)-treated Aβ in the absence and presence of O_2, analyzed by ESI–MS and ESI–MS^2. (*A* and *B*) ESI–MS spectra of the +3-charged monomeric Aβ species from the samples of Cu(I)-added $Aβ_{40}$ incubated with and without **L1** under anaerobic and aerobic conditions. (*C* and *D*) ESI–MS^2 spectra of the covalent adduct (1,475 *m/z*) and the singly oxidized $Aβ_{40}$ (1,449 *m/z*) produced upon reaction of Cu(I)-treated Aβ with **L1** under aerobic conditions. Conditions were as follows: [$Aβ_{40}$] = 100 μM; [Cu(I)] = 100 μM; [**L1**] = 500 μM; incubation for 1 h; 20 mM ammonium acetate, pH 7.2; 37 °C; no agitation. The samples were diluted with H_2O by 10 fold under aerobic conditions prior to injection to the mass spectrometer.

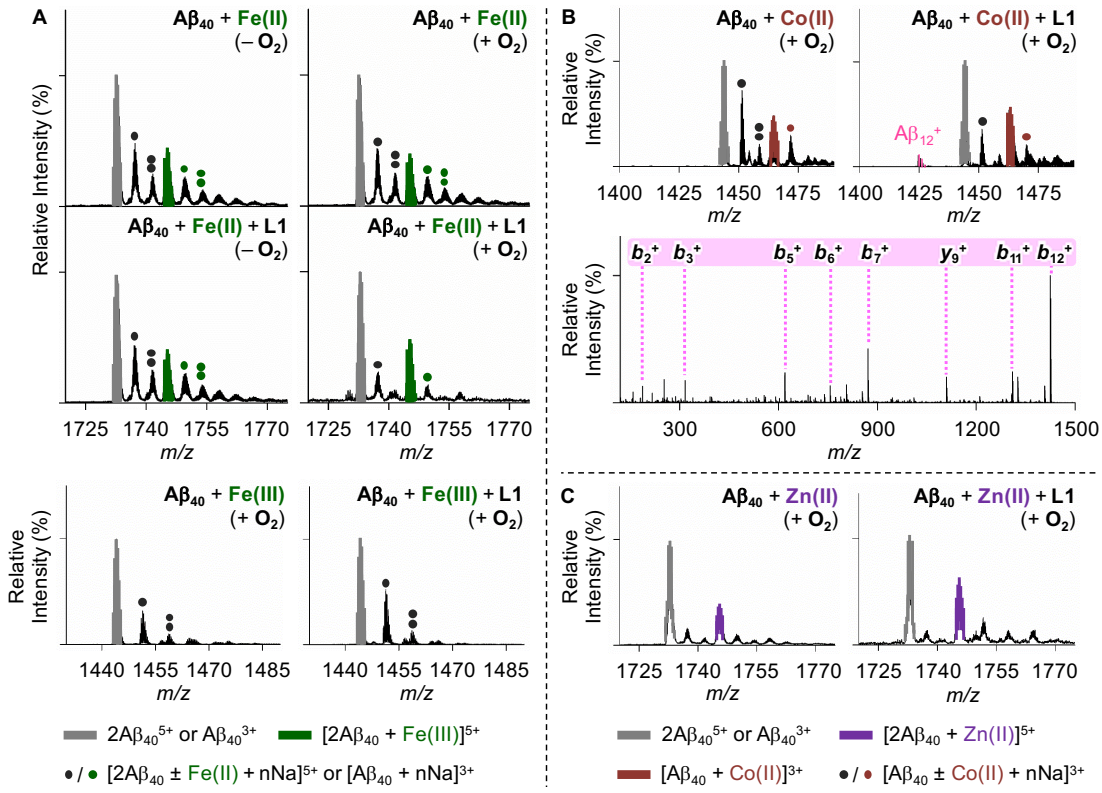

Fig. S18. Interactions of **L1** with Fe(II/III)-, Co(II)-, and Zn(II)-added Aβ in the absence and presence of O_2, analyzed by ESI–MS. (*A*) Spectra of Fe(II)- or Fe(III)-treated $A\beta_{40}$ upon incubation with **L1** under anaerobic or aerobic conditions. (*B*) ESI–MS spectra of the +3-charged Co(II)-added $A\beta_{40}$ monomer incubated with and without **L1** under aerobic conditions. The ESI–MS^2 spectrum of the selected ion at 1,424 *m/z* presents the formation of a fragmented $A\beta_{40}$, $A\beta_{12}$, upon reaction of **L1** with Co(II)-added $A\beta_{40}$. The magenta box indicates *b* and *y* fragments corresponding to $A\beta_{12}$. (*C*) Spectra of Zn(II)-added $A\beta_{40}$ upon treatment of **L1** under aerobic conditions. Conditions were as follows: [$A\beta_{40}$] = 100 μM; [M(II) or M(III)] = 100 μM; [**L1**] = 500 μM; incubation for 1 h; 20 mM ammonium acetate, pH 7.2; 37 °C; no agitation. The samples were diluted with H_2O by 10 fold prior to injection to the mass spectrometer. Note that Co(II)-bound $A\beta_{40}$ monomer was observed under our experimental conditions, but Fe(II)-, Fe(III)-, and Zn(II)-bound $A\beta_{40}$ monomer was not detected.

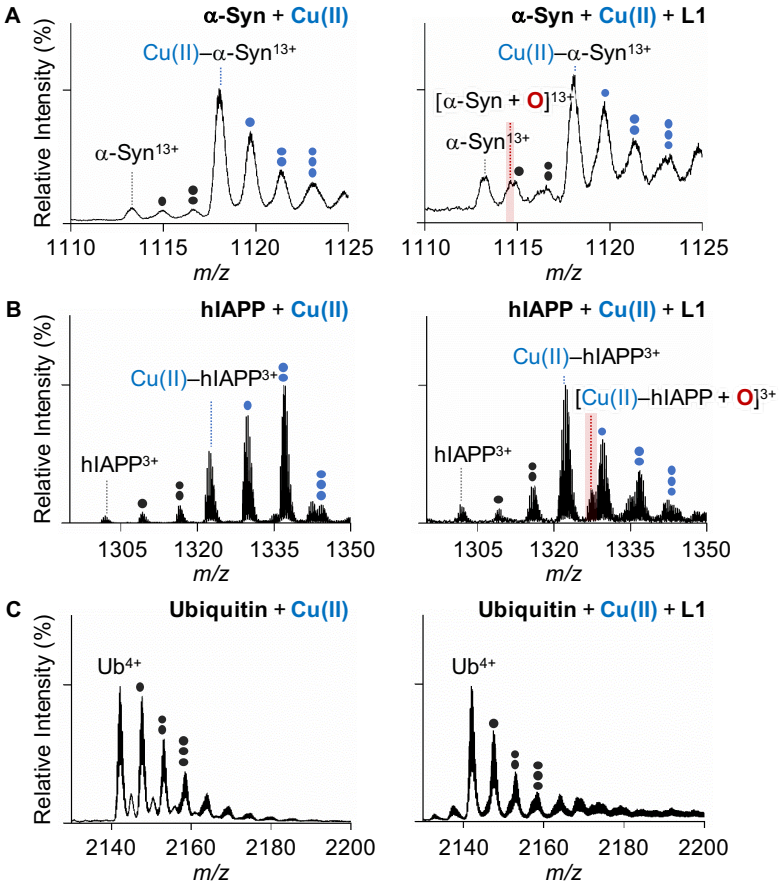

Fig. S19. ESI–MS analysis of Cu(II)-added α-synuclein (α-Syn), human islet amyloid polypeptide (hIAPP), and ubiquitin with treatment of **L1**. (*A*–*C*) Spectra of α-Syn, hIAPP, and ubiquitin incubated with Cu(II) and/or **L1**. Na^+ adducts of proteins with or without Cu(II) are shown with blue and black dots. Conditions were as follows: [proteins] = 100 μM; [$CuCl_2$] = 100 μM; [**L1**] = 500 μM; incubation for 1 h; 20 mM ammonium acetate, pH 7.2; 37 °C; no agitation. The samples were diluted with H_2O by 10 fold prior to injection to the mass spectrometer.

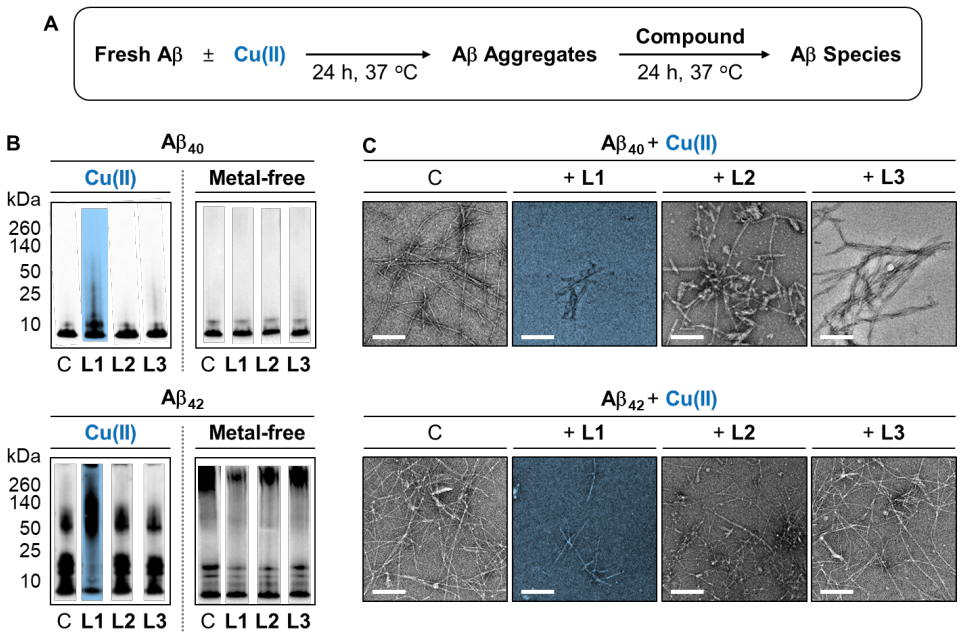

Fig. S20. Impact of **L1**–**L3** on preformed Cu(II)-bound and metal-free Aβ aggregates. (*A*) Scheme of the disaggregation experiments. (*B*) Analysis of the size distribution of the resultant $A\beta_{40}$ (top) and $A\beta_{42}$ (bottom) species by the gel/Western blot using an anti-Aβ antibody (6E10). Lanes are as follows: C, Aβ with or without $CuCl_2$; **L1**, C with **L1**; **L2**, C with **L2**; **L3**, C with **L3**. The original gel images are presented in Fig. S24*B*. (*C*) Morphologies of the Cu(II)-treated $A\beta_{40}$ (top) and $A\beta_{42}$ (bottom) aggregates from (*B*), monitored by TEM. Scale bars, 200 nm. Conditions were as follows: [Aβ] = 25 μM; [$CuCl_2$] = 25 μM; [compound] = 50 μM; 37 °C; constant agitation.

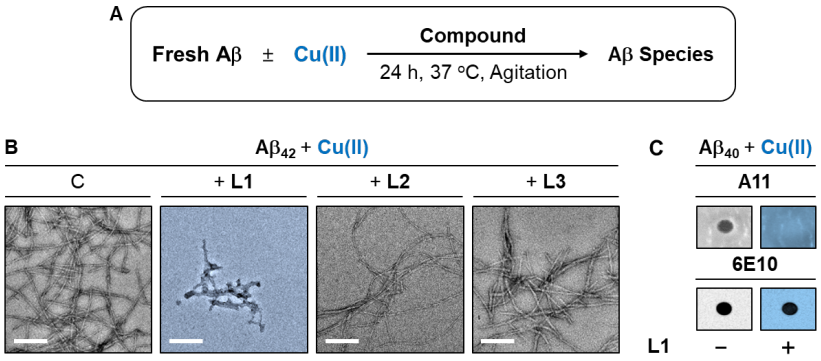

Fig. S21. Analysis of the Cu(II)–Aβ samples treated with or without **L1** by TEM or the dot blot assay. (*A*) Scheme of the inhibition experiments. (*B*) Morphologies of the resultant $A\beta_{42}$ aggregates from the inhibition experiments, monitored by TEM. Scale bars, 200 nm. Conditions were as follows: [Aβ], 25 μM; [compound], 50 μM; 37 °C; constant agitation. (*C*) Dot blots of Cu(II)-added $A\beta_{40}$ incubated with and without **L1** using an anti-oligomer antibody (A11) and an anti-Aβ antibody (6E10). Conditions were as follows: [$A\beta_{40}$] = 100 μM; [$CuCl_2$] = 100 μM; [compound] = 200 μM; 37 °C; constant agitation.

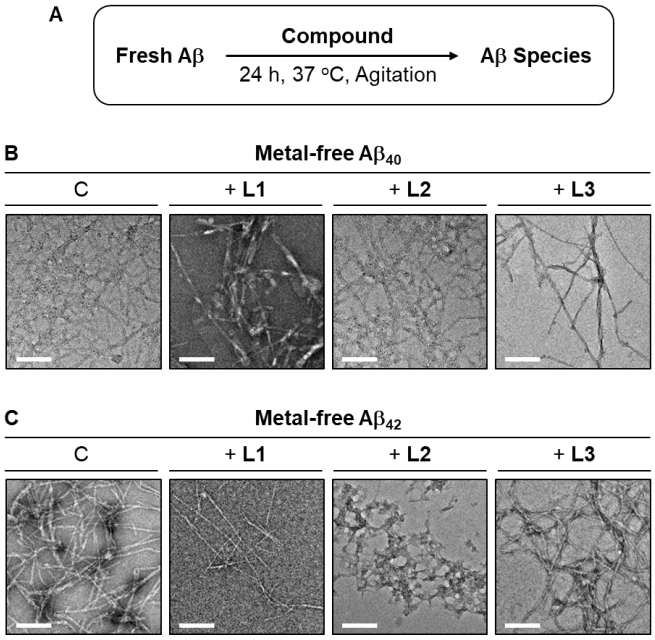

Fig. S22. TEM images of the resultant metal-free $A\beta_{40}$ and $A\beta_{42}$ aggregates generated with treatment with **L1**–**L3** from the inhibition experiments. (*A*) Scheme of the inhibition experiments. (*B* and *C*) Morphologies of the resultant $A\beta_{40}$ and $A\beta_{42}$ aggregates, monitored by TEM. Scale bars, 200 nm. Conditions were as follows: [Aβ] = 25 μM; [compound] = 50 μM; 37 °C; constant agitation.

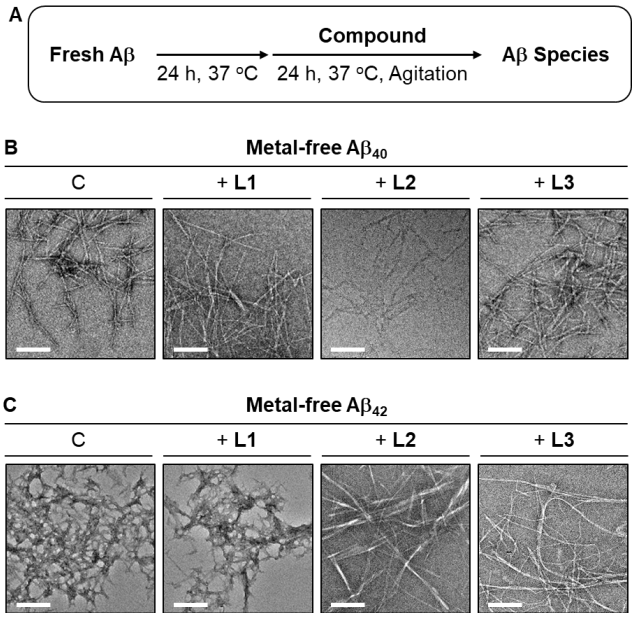

Fig. S23. TEM images of the resultant metal-free $A\beta_{40}$ and $A\beta_{42}$ aggregates formed upon incubation with **L1**–**L3** from the disaggregation experiments. (*A*) Scheme of the disaggregation experiments. (*B* and *C*) Morphologies of the resultant $A\beta_{40}$ and $A\beta_{42}$ aggregates, monitored by TEM. Scale bars, 200 nm. Conditions were as follows: [Aβ] = 25 μM; [compound] = 50 μM; 37 °C; constant agitation.

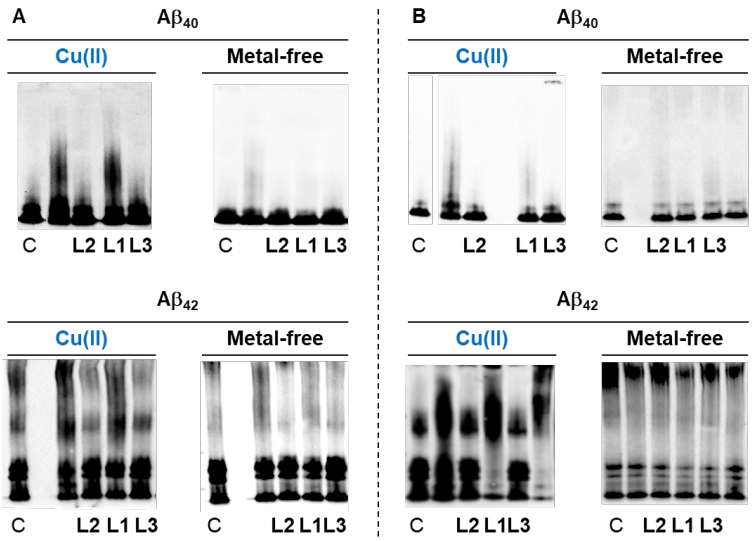

Fig. S24. Original gel images from the (*A*) inhibition (Fig. 4*B*) and (*B*) disaggregation (Fig. S20*B*) experiments.

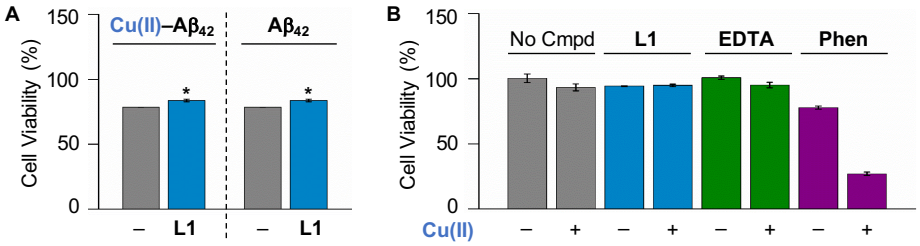

Fig. S25. Viability of SH-SY5Y cells treated with Aβ, Cu(II), and compounds. (*A*) Cytotoxicity of Cu(II)–$A\beta_{42}$ and metal-free $A\beta_{42}$ that were incubated with **L1**. (*B*) Cytotoxicity of **L1**, **EDTA**, and **phen** in the absence and presence of Cu(II). Cell viability, determined by the MTT assay, was calculated in comparison to that obtained upon treatment with an equivalent amount of DMSO. Conditions were as follows: [Aβ] = 10 μM; [$CuCl_2$] = 10 μM; [compound] = 10 μM. *$P < 0.05$ by Student's *t* test.

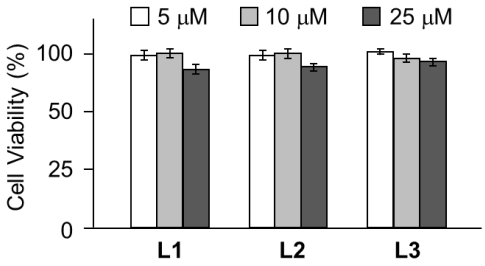

Fig. S26. Cytotoxicity of **L1**–**L3**, determined by the MTT assay. Cell viability was calculated in comparison to that obtained upon treatment with an equivalent amount of DMSO. Error bars represent the standard deviation from three independent experiments.

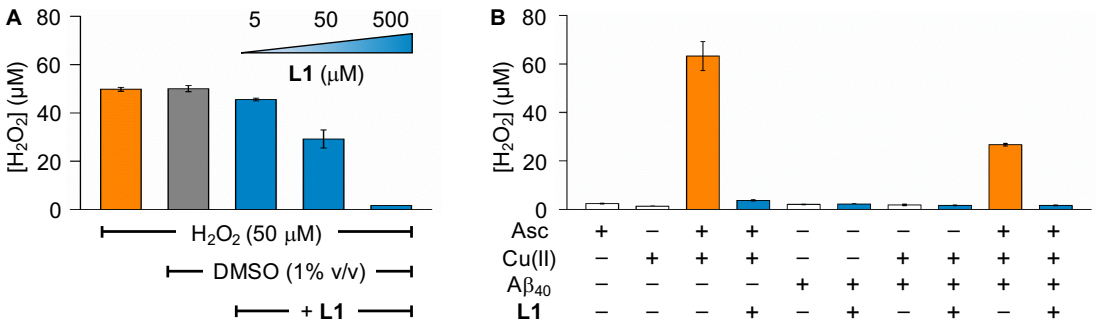

Fig. S27. Impact of **L1** on H_2O_2 or H_2O_2 generated via Fenton-like reactions of Cu(I/II) or Cu(I/II)–Aβ_{40}. (*A*) Amount of H_2O_2 with and without treatment of **L1**, measured by an Amplex Red H_2O_2/peroxidase assay. Conditions were as follows: [H_2O_2] = 50 μM; [**L1**] = 5, 50, and 500 μM (DMSO 1% v/v). (*B*) Concentration of H_2O_2 in the samples [*L*-ascorbate only (Asc); Cu(II) only; *L*-ascorbate + Cu(II); *L*-ascorbate + Cu(II) + **L1**; Aβ_{40} only; Aβ_{40} + **L1**; Cu(II) + Aβ_{40}; Cu(II) + Aβ_{40} + **L1**; *L*-ascorbate + Cu(II) + Aβ_{40}; *L*-ascorbate + Cu(II) + Aβ_{40} + **L1**], detected by an Amplex Red H_2O_2/peroxidase assay. Conditions were as follows: [Aβ_{40}] = 25 μM; [$CuCl_2$] = 25 μM; [*L*-ascorbate] = 1 mM; [**L1**] = 50 μM (DMSO 1% v/v).

References

1. S. Lee *et al.*, Rational design of a structural framework with potential use to develop chemical reagents that target and modulate multiple facets of Alzheimer's disease. *J. Am. Chem. Soc.* **136**, 299–310 (2015).
2. J.-S. Choi, J. J. Braymer, R. P. Nanga, A. Ramamoorthy, M. H. Lim, Design of small molecules that target metal–Aβ species and regulate metal-induced Aβ aggregation and neurotoxicity. *Proc. Natl. Acad. Sci. U. S. A.* **107**, 21990–21995 (2010).
3. J. S. Derrick *et al.*, A redox-active, compact molecule for cross-linking amyloidogenic peptides into nontoxic, off-pathway aggregates: in vitro and in vivo efficacy and molecular mechanisms. *J. Am. Chem. Soc.* **137**, 14785–14797 (2015).
4. L. Di, E. H. Kerns, K. Fan, O. J. McConnell, G. T. Carter, High throughput artificial membrane permeability assay for blood-brain barrier. *Eur. J. Med. Chem.* **38**, 223–232 (2003).
5. A. Avdeef *et al.*, PAMPA–critical factors for better predictions of absorption. *J. Pharm. Sci.* **96**, 2893–2909 (2007).
6. S. S. Hindo *et al.*, Small molecule modulators of copper-induced Aβ aggregation. *J. Am. Chem. Soc.* **131**, 16663–16665 (2009).
7. H. J. Lee *et al.*, Structural and mechanistic insights into development of chemical tools to control individual and inter-related pathological features in Alzheimer's disease. *Chem. Eur. J.* **23**, 2706–2715 (2017).
8. M. W. Beck *et al.*, A rationally designed small molecule for identifying an in vivo link between metal–amyloid-β complexes and the pathogenesis of Alzheimer's disease. *Chem. Sci.* **6**, 1879–1886 (2015).
9. S.-J. Hyung *et al.*, Insights into antiamyloidogenic properties of the green tea extract (–)-epigallocatechin-3-gallate toward metal-associated amyloid-β species. *Proc. Natl. Acad. Sci. U. S. A.* **110**, 3743–3748 (2013).
10. A. Micsonai *et al.*, Accurate secondary structure prediction and fold recognition for circular dichroism spectroscopy. *Proc. Natl. Acad. Sci. U. S. A.* **112**, E3095–E3103 (2015).
11. D. D. Mruk, C. Y. Cheng, Enhanced chemiluminescence (ECL) for routine immunoblotting: an inexpensive alternative to commercially available kits. *Spermatogenesis* **1**, 121–122 (2011).